

Complex magnetic phases of $\text{Ca}_{1-x}\text{Na}_x\text{V}_2\text{O}_4$ clarified by muon-spin spectroscopy

Jun Sugiyama,^{1,*} Yutaka Ikeda,¹ Tatsuo Goko,² Eduardo J. Ansaldo,² Jess H. Brewer,^{2,3} Peter L. Russo,² Kim H. Chow,⁴ and Hiroya Sakurai⁵

¹*Toyota Central Research and Development Laboratories Inc., Nagakute, Aichi 480-1192, Japan*

²*TRIUMF, 4004 Wesbrook Mall, Vancouver, British Columbia, Canada V6T 2A3*

³*CIfAR and Department of Physics and Astronomy, University of British Columbia, Vancouver, British Columbia, Canada V6T 1Z1*

⁴*Department of Physics, University of Alberta, Edmonton, Alberta, Canada T6G 2G7*

⁵*National Institute for Materials Science, Namiki, Tsukuba, Ibaraki 305-0044, Japan*

(Received 3 October 2008; published 5 December 2008)

The microscopic magnetic nature of $\text{Ca}_{1-x}\text{Na}_x\text{V}_2\text{O}_4$ with $0 \leq x \leq 1$ has been investigated by a positive muon-spin spectroscopy ($\mu^+\text{SR}$) using powder samples for temperatures down to 1.8 K. Static antiferromagnetic (AF) order is observed for the metallic compounds with $x \geq 9.3/12$ as well as for NaV_2O_4 and insulating CaV_2O_4 . A variety of phases was also found to appear as a function of x and/or temperature. Combining with the pressure dependence of static AF order, the precise analysis of the zero-field $\mu^+\text{SR}$ spectrum suggests the rearrangement of spin order on the V_2O_4 chain with temperature for the metallic compounds.

DOI: [10.1103/PhysRevB.78.224406](https://doi.org/10.1103/PhysRevB.78.224406)

PACS number(s): 76.75.+i, 75.25.+z, 75.50.Ee, 75.50.Lk

I. INTRODUCTION

The title compounds are members of the broad class of quasi-one-dimensional (quasi-1D) spin systems for which there are extensive experimental and theoretical interests.¹⁻³ This is due to the variety of fascinating phenomena encountered in quasi-1D materials, such as unconventional magnetic ground states,⁴⁻⁶ quantum magnetism,^{7,8} as well as pressure induced perhaps eccentric superconductivity.⁹ The physics behind these phenomena is governed by the strong spin-spin coupling along one direction, ostensibly parallel to the 1D direction, together with a much weaker coupling along the other directions. The $(\text{Ca}, \text{Na})\text{V}_2\text{O}_4$ compounds are particularly interesting as examples of relatively simple $S=1$ Haldane systems,¹⁰⁻¹² with the characteristic feature of having (1D) “zig-zag” (zz) chains in the structure.

Both CaV_2O_4 and NaV_2O_4 belong to a CaFe_2O_4 -type orthorhombic structure with a space group $Pnma$, in which V_2O_4 double chains, i.e., zig-zag chains formed by a network of edge-sharing VO_6 octahedra align along the b axis so as to make an irregular hexagonal 1D channel. CaV_2O_4 is synthesized by a conventional solid-state reaction technique.¹³ Since the V ions are in a +3 state with $S=1$ (t_{2g}^2), the ground state of CaV_2O_4 was thought to be a gapless chiral-ordered state, which is predicted for the $S=1$ zig-zag spin system.¹² However, recent NMR results confirmed the existence of long-range antiferromagnetic (AF) order below $T_N=78$ K.¹⁴ This is consistent with past neutron measurements, in which two different AF substructures coexist in the $a \times 2b \times 2c$ AF supercell, and each superstructure is collinear which is roughly parallel to the b axis.¹⁵

On the other hand, NaV_2O_4 is a material recently prepared by a high-pressure technique.¹⁶ Intriguingly, because of a mixed-valence state of the V ions (+3.5), NaV_2O_4 exhibits metallic conductivity down to 40 mK, while susceptibility (χ) measurements indicate an AF transition with $T_N=140$ K. Magnetic anisotropy measurements using single-crystal samples suggested that the interchain interaction is AF, while the intrachain interaction is ferromagnetic (FM),

as in the case of quasi-1D cobalt oxides.¹⁷ The AF structure of NaV_2O_4 has—to the authors’ knowledge—never been investigated with NMR, neutron, or positive muon-spin spectroscopy ($\mu^+\text{SR}$) measurements. As a result, the mechanism of the metallic AF order is still unknown.

Subsequently, $\text{Ca}_{1-x}\text{Na}_x\text{V}_2\text{O}_4$ was prepared in the whole x range under a 6 GPa high-pressure apparatus.¹⁸ Based on resistivity (ρ), χ , and heat-capacity (C_p) measurements, a macroscopic phase diagram of $\text{Ca}_{1-x}\text{Na}_x\text{V}_2\text{O}_4$ was determined as follows: the compounds with $x \leq 5/12$ are insulating below 350 K, while those with $5/12 < x \leq 0.78$ ($\sim 9.3/12$) exhibit a transition from a high- T metallic phase to a low- T insulator phase at T_{mi} ($=320$ K for $x=6/12$ and 110 K for $x=0.78$). The compounds with $x > 0.78$, on the other hand, are metallic down to the lowest T measured. Although the $\chi(T)$ curve exhibits a typical anomaly at $T_N=78$ K for CaV_2O_4 , such anomaly is likely to disappear for the phase with $0 < x \leq 0.78$. The $\chi(T)$ curve also shows a broad maximum at 300 K ($=T_{\text{max}}$) for $x=0$. T_{max} increases slowly with x and reaches its highest value (320 K) at $x=1/3$ then rapidly decreases down to 120 K with further increasing x up to 0.78. Thus, T_{max} corresponds to T_{mi} in the x range between $4/12$ and 0.78. For $\text{Ca}_{0.22}\text{Na}_{0.78}\text{V}_2\text{O}_4$, T_N is clearly observed again at ~ 100 K in the $\chi(T)$ curve. Then, T_N increases linearly with x and reaches 140 K for NaV_2O_4 . In addition, precise $\chi(T)$ measurements showed the existence of three different AF phases in the x range above 0.78.

Since the microscopic nature is sometimes different from the macroscopic one, in this paper, we report our $\mu^+\text{SR}$ results on polycrystalline samples of $\text{Ca}_{1-x}\text{Na}_x\text{V}_2\text{O}_4$ with $x=0, 1/12, 2/12, 4/12, 6/12, 8/12, 9.3/12, 10/12, 11/12$, and 1; including pressure effects using a special sample cell to apply hydrostatic pressure on the samples. We demonstrate the existence of a variety of phases as a function of x in $\text{Ca}_{1-x}\text{Na}_x\text{V}_2\text{O}_4$. In particular, the pressure dependence of static AF order in the metallic samples suggests the essential role of the competition between intrachain and interchain interactions on the appearance of the three AF phases.

II. EXPERIMENT

Polycrystalline samples of $\text{Ca}_{1-x}\text{Na}_x\text{V}_2\text{O}_4$ were prepared by a solid-state reaction technique under a pressure of 6 GPa using CaV_2O_4 , $\text{Na}_4\text{V}_2\text{O}_7$, and V_2O_3 powders as starting materials. A mixture of the three powders was packed in an Au capsule then heated at 1300 °C for 1 h and finally quenched to ambient T . A powder x-ray diffraction (XRD) analysis showed that all the samples were almost single phase with an orthorhombic system of space group $Pnma$ at ambient T . dc- χ measurements showed that all our samples have almost the same T dependence as that in the previous report.¹⁸ The preparation and characterization of the samples have been reported in greater detail elsewhere.¹⁸ The μ^+ SR experiments were performed on both the M20 surface muon beam line and the M9B decay muon beam line at TRIUMF using an experimental setup and techniques described elsewhere.¹⁹ For the high-pressure μ^+ SR measurements, a piston cylindrical cell made of MP35 alloy was used to apply pressure up to 1.7 GPa. Three disks of the sample were stacked in the sample space (6 mm diameter and 10 mm length) of the cell. Daphne oil was used as the medium to apply hydrostatic pressure to the sample.

III. RESULTS

Figure 1 shows T dependence of the normalized weak transverse-field (wTF) asymmetry ($N_{A_{\text{TF}}}$), which is roughly proportional to the volume fraction of paramagnetic phases in the sample, for $\text{Ca}_{1-x}\text{Na}_x\text{V}_2\text{O}_4$ in the whole x range. A sharp AF transition is observed for $x=0, 6/12, 8/12, 10/12, 11/12$, and 1 as the $N_{A_{\text{TF}}}(T)$ curve exhibits a step-like change from 1 to 0 at a certain $T(=T_N)$ with decreasing T . In contrast, the samples with $0 < x < 4/12$ are likely to be a mixture of CaV_2O_4 and the $x \sim 6/12$ phase, although they were identified structurally as a single phase by an XRD analysis at ambient T .¹⁸ This would imply the microscopic phase separation at low T for these samples. Also, the $x=9.3/12$ sample is clearly found to be a mixture of the two phases; that is, the $x=8/12$ phase and the phase with $T_N \sim 96$ K, which should correspond to the compound with the lowest x in the metallic AF region. Combining with the result of zero-field (ZF) μ^+ SR measurements described later, a magnetic phase diagram is determined as seen in Fig. 1(c), which is very different from that reported by macroscopic measurements.¹⁸ In particular, the AF phase with wide field distribution, i.e., a spin-glass-like phase, was found below $T_N \sim 10$ K in the x range between $6/12$ and $9.3/12$. Furthermore, since $N_{A_{\text{TF}}}$ for all the samples reaches its maximum value ($=1$) above the vicinity of T_N , T_{max} in the $\chi(T)$ curve at high T is not magnetic in origin.

Figures 2(a) and 2(b) show the ZF spectrum for NaV_2O_4 and CaV_2O_4 at the lowest T measured and below the vicinity of T_N . Interestingly, the ZF spectrum for NaV_2O_4 at 131 K exhibits a simple oscillation, while the one at 1.8 K includes multioscillating signals. For CaV_2O_4 , however, the ZF spectrum consists of mainly two oscillating signals at both T 's. The unique T dependence of the ZF spectrum is easily understandable in Figs. 2(c) and 2(d), which displays the Fou-

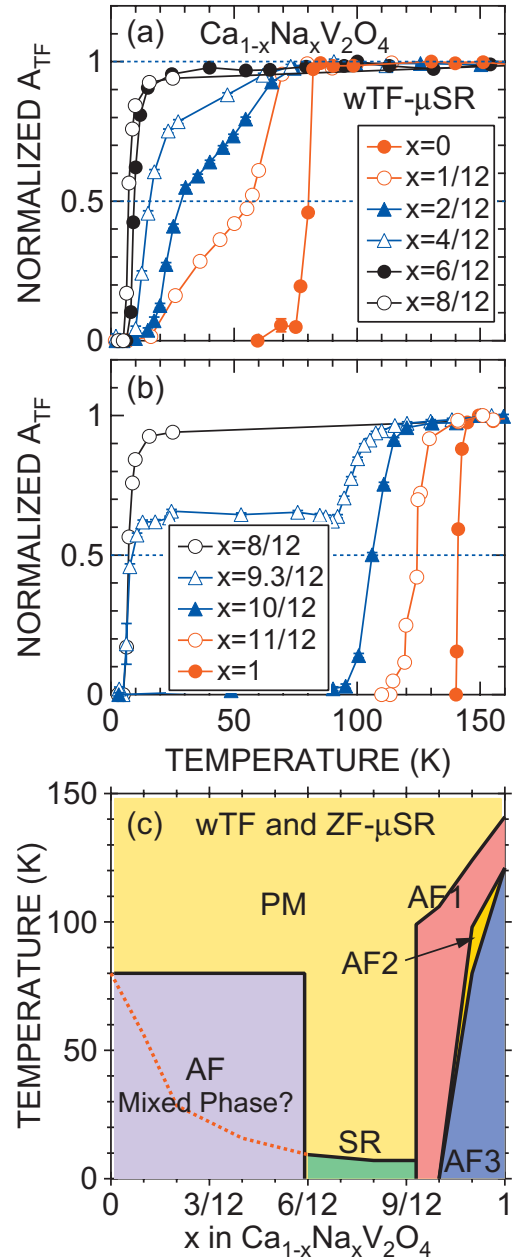


FIG. 1. (Color) T dependence of the normalized wTF asymmetry $N_{A_{\text{TF}}}$ for $\text{Ca}_{1-x}\text{Na}_x\text{V}_2\text{O}_4$ with (a) $x=0-8/12$, (b) $x=8/12-1$, and (c) a tentative phase diagram determined by both wTF and ZF μ^+ SR. PM means paramagnetic phase; AF, AF1, AF2, and AF3 means static antiferromagnetic ordered phases, and SR means short-range AF ordered phase. A red broken line in (c) represents the T at which $N_{A_{\text{TF}}}=0.5$.

rier transform of the ZF spectrum as a function of T . For NaV_2O_4 , the ZF spectrum consists of mainly four signals below 120 K and one signal above 125 K. But, for CaV_2O_4 , the ZF spectrum consists of two signals with significant amplitudes and an additional two signals with smaller amplitude in the entire T range below T_N . The ZF- μ^+ SR spectra below T_N were therefore fitted with a sum of four oscillating signals and one slow exponentially relaxing signal due to the “1/3 tail” caused by the field component parallel to the initial muon-spin polarization,

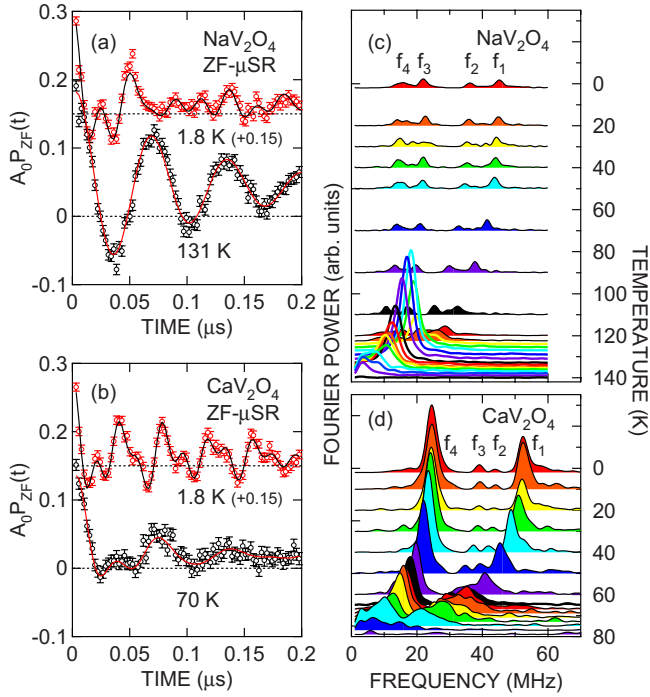


FIG. 2. (Color online) (a) [(b)] Variation in ZF- μ^+ SR time spectrum by T and (c) [(d)] T dependence of the Fourier transform of the ZF- μ^+ SR time spectrum for NaV_2O_4 [CaV_2O_4]. Top two spectra in (a) and (b) are offset by 0.15 for clarity of display. f_i in (c) and (d) indicates the frequency of the four oscillating signals.

$$A_0 P_{\text{ZF}}(t) = \sum_{i=1}^4 A_{\text{AF},i} \cos(\omega_{\mu,i} t + \phi) \exp(-\lambda_i t) + A_{\text{tail}} \exp(-\lambda_{\text{tail}} t), \quad (1)$$

where ϕ is the initial phase of the precession, A_i are the asymmetries, λ_i ($i=1-4$) are exponential relaxation rates, and $\omega_{\mu,i}$ are the muon Larmor frequencies of the four signals. The number of oscillating components was found to be dependent on T and x .

Figure 3 shows the T dependence of the muon-precession frequencies ($f_i \equiv \omega_{\mu,i}/2\pi$) for $x=1, 11/12, 10/12$, and 0. For NaV_2O_4 , as T increases from 1.8 K, the four f_i 's decrease slowly up to ~ 50 K then decrease more rapidly with further increasing T and then finally merge into one signal at 120 K. This latter signal drops rapidly with increasing its slope and finally reaches 0 at 140 K ($=T_{N1}$). This suggests the existence of another AF transition at ~ 120 K ($=T_{N3}$). In addition, since $\phi = -11 \pm 3^\circ$ at 1.8 K, the period of AF order is likely to be commensurate with the lattice.²⁰ For the $x=11/12$ sample, as T increases from 1.8 K, the number of f_i decreases from four to two at 88 K ($=T_{N3}$) and then to one at 100 K ($=T_{N2}$) and finally the oscillating signal disappears above 130 K ($=T_{N1}$). In contrast, for the $x=10/12$ sample, only one f is observed down to 1.8 K ($T_{N1}=110$ K), whereas four (two major and two minor) f_i 's are observed for CaV_2O_4 with $T_N=78$ K.

Finally, wTF- μ^+ SR measurements under a pressure (P) of 1.7 GPa showed a decrease in T_{N1} by ~ 10 K for NaV_2O_4

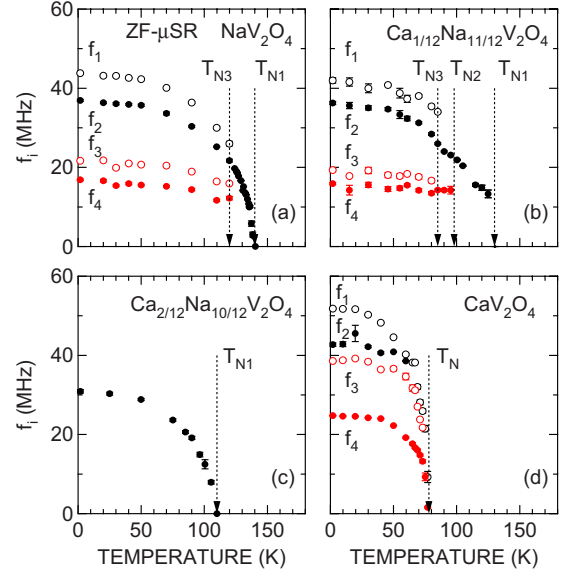


FIG. 3. (Color online) T dependence of the muon-precession frequencies (f_i) for (a) NaV_2O_4 , (b) $\text{Ca}_{1/12}\text{Na}_{11/12}\text{V}_2\text{O}_4$, (c) $\text{Ca}_{2/12}\text{Na}_{10/12}\text{V}_2\text{O}_4$, and (d) CaV_2O_4 . There are two AF phases for NaV_2O_4 ; namely, AF1 at $T_{N3} < T \leq T_{N1}$ and AF3 at $T \leq T_{N3}$, whereas $\text{Ca}_{1/12}\text{Na}_{11/12}\text{V}_2\text{O}_4$ has three AF Phases; AF1 at $T_{N2} < T \leq T_{N1}$, AF2 at $T_{N3} < T \leq T_{N2}$, and AF3 at $T \leq T_{N3}$. These AF phases are shown in Fig. 1(c).

and by ~ 8 K for the $x=10/12$ sample (see Fig. 4). In contrast, the applied P is found to stabilize the AF3 phase: the ZF spectrum at 3 K under 1.7 GPa consists of the four oscillating signals, i.e., indicating the appearance of the AF3 phase in $\text{Ca}_{2/12}\text{Na}_{10/12}\text{V}_2\text{O}_4$, whereas the AF1 phase is stable at ambient P down to 1.8 K. The AF3 phase region (T_{N3}) is also enhanced by P for NaV_2O_4 .

IV. DISCUSSION

Electrostatic potential calculations suggest that there are two possible muon sites (I and III) near the O^{2-} ions in the crystallographic lattice of both CaV_2O_4 and NaV_2O_4 at ambient T (see Fig. 5). Assuming the proposed AF spin structure for CaV_2O_4 ,^{14,15,21} i.e., AF order along the two 1D legs in the zz chain, and AF order between the zz chains [Figs. 5(b) and (b')], dipole field calculations indicate the existence of two distinct internal magnetic fields ($H_{\text{int}1}$ and $H_{\text{int}4}$) with the same amplitude. We find that $H_{\text{int}1}/\mu_{\text{V}} = 2.87(9)$ kOe/ μ_{B} , $H_{\text{int}4}/\mu_{\text{V}} = 1.75(15)$ kOe/ μ_{B} , and $H_{\text{int}1}/H_{\text{int}4} = 1.6(2)$, where H_{int} is proportional to the ordered moment (μ_{V}) and $H_{\text{int}} \times 13.554(\text{kHz/Oe}) = f$. Ignoring the two minor components (f_2 and f_3), since the observed $f_1/f_4 = 2.09(1)$ [see Fig. 3(d)], the calculated result is consistent with the experimental one to within 20% error. Furthermore, the absolute values of f_1 and f_4 enable us to estimate that $\mu_{\text{V}}(1.8 \text{ K}) = 1.19(14)\mu_{\text{B}}$, which is in good agreement with the proposed value from the neutron measurement [$1.06(6)\mu_{\text{B}}$].^{15,21}

In order to explain the unique H_{int} for NaV_2O_4 in the AF1 phase (i.e., between T_{N1} and T_{N3}) together with the metallic behavior down to the lowest T measured, we propose that the

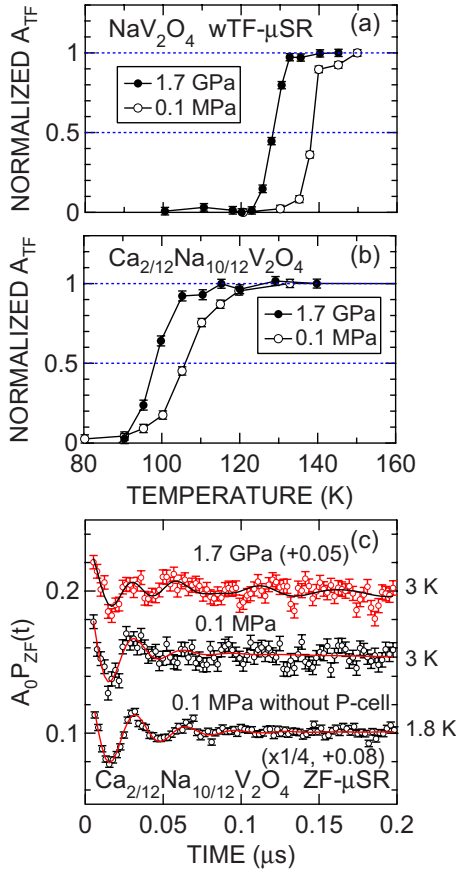


FIG. 4. (Color online) T dependence of $N_{A_{TF}}$ at 0.1 MPa ($=1$ bar) and 1.7 GPa for (a) NaV_2O_4 and (b) $\text{Ca}_{2/12}\text{Na}_{10/12}\text{V}_2\text{O}_4$ and (c) the variation in ZF- μ^+ SR time spectrum for $\text{Ca}_{2/12}\text{Na}_{10/12}\text{V}_2\text{O}_4$ by pressure. The spectrum without the P cell is also plotted for comparison in (c).

V spins are ordered ferromagnetically along the zz chain but antiferromagnetically between the adjacent zz chains [see Figs. 5(c) and (c')], if we assume the commensurate AF order. Dipole field calculations using this model reproduce a unique H_{int} with $2.40(2)$ kOe/ μ_B . Note that in contrast to the AF1 phase, we propose that in the AF3 phase one FM ordered 1D leg couples with the other leg antiferromagnetically in the zz chain and each zz chain also couples antiferromagnetically [see Figs. 5(d) and (d')]. The FM coupling along the leg should be stronger than the AF coupling between the two legs,¹⁶ resulting in metallic behavior even in the AF3 phase. Dipole field calculations yield four different H_{int} 's with the same amplitude, i.e., 3.02, 2.79, 2.41, and 2.15 kOe/ μ_B for $i=1-4$, respectively. The ratio between them ($H_{\text{int}i}/H_{\text{int}4}$) is smaller than the experimental result, i.e., $f_i/f_4=2.59, 2.20$, and 1.28 for $i=1-3$. This discrepancy is probably due to a small deviation of the spin arrangement between the zz chains from the proposed one [Fig. 5(d')]. The magnitude of μ_V is estimated as $0.82(14)\mu_B$ at 1.8 K.

In principle, the drastic change in T_{N3} could also be due to a structural change in NaV_2O_4 , although there is no evidence of structural phase transitions—including charge ordering—in the $\rho(T)$ and $C_p(T)$ curves at T_{N3} . This implies that such a structural change is a small spatial displacement

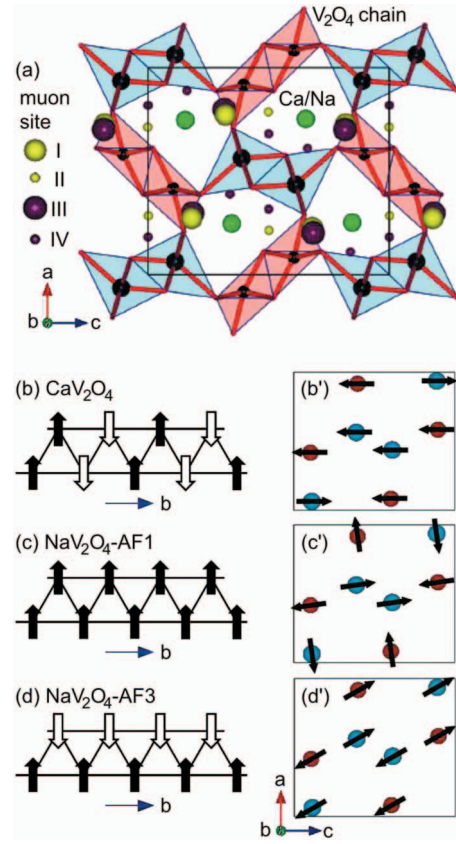


FIG. 5. (Color) (a) Possible muon sites in the $\text{Ca}_{1-x}\text{Na}_x\text{V}_2\text{O}_4$ lattice, (b) and (b') proposed spin structure for CaV_2O_4 , (c) and (c') for AF1 phase of NaV_2O_4 , and (d) and (d') for AF3 phase of NaV_2O_4 . According to electrostatic potential calculations, sites I and III are most stable among the four sites. In (b'), each spin is parallel or antiparallel to the c axis, while each spin is canted by 7.5° and 30° from the c axis in (c') and (d'), respectively.

of O^{2-} ions at T_{N3} , leading to the change in the μ^+ sites and the number of f_i .²² However, such displacements are expected to be suppressed by P , in contrast to the present result. Therefore, rearrangement of spin order at T_{N3} is likely to be the more reasonable mechanism for the appearance of the AF3 phase.

In summary, our systematic study on $\text{Ca}_{1-x}\text{Na}_x\text{V}_2\text{O}_4$ yields insights into the 1D zig-zag chain compound; namely, a microscopic magnetic phase diagram was determined by μ^+ SR which is quite different from that proposed by macroscopic measurements particularly in the x range below 0.78 ($\sim 9.3/12$). These studies emphasize the importance of microscopic experimental studies for the full understanding of magnetic systems. As an example of the clarity of the results, the existence of the three AF phases were thus confirmed for $\text{Ca}_{1-x}\text{Na}_x\text{V}_2\text{O}_4$ with $x \geq 0.78$.

ACKNOWLEDGMENTS

We thank the staff of TRIUMF for the help with the μ^+ SR experiments. Y.I. and J.S. are partially supported by the

KEK-MSL Inter-University Program for Oversea Muon Facilities. J.H.B. is supported at UBC by Cifar, NSERC, and (through TRIUMF) by NRC of Canada. K.H.C. is supported by NSERC and (through TRIUMF) by NRC of Canada, and

H.S. is supported by WPI Initiative on Materials, Nanoarchitectonics of MEXT, Japan. This work is also supported by the Grant-in-Aid for Scientific Research (B) under Grant No. 19340107 of MEXT, Japan.

*e0589@mosk.tytlabs.co.jp

- ¹T. Masuda, A. Zheludev, H. Manaka, L.-P. Regnault, J.-H. Chung, and Y. Qiu, Phys. Rev. Lett. **96**, 047210 (2006).
- ²L. Mihály, B. Dóra, A. Ványolos, H. Berger, and L. Forró, Phys. Rev. Lett. **97**, 067206 (2006).
- ³A. A. Zvyagin and S.-L. Drechsler, Phys. Rev. B **78**, 014429 (2008).
- ⁴J. Sugiyama, H. Nozaki, J. H. Brewer, E. J. Ansaldo, T. Takami, H. Ikuta, and U. Mizutani, Phys. Rev. B **72**, 064418 (2005).
- ⁵J. Sugiyama, H. Nozaki, Y. Ikedo, K. Mukai, D. Andreica, A. Amato, J. H. Brewer, E. J. Ansaldo, G. D. Morris, T. Takami, and H. Ikuta, Phys. Rev. Lett. **96**, 197206 (2006).
- ⁶J. Sugiyama, H. Nozaki, Y. Ikedo, P. L. Russo, K. Mukai, D. Andreica, A. Amato, T. Takami, and H. Ikuta, Phys. Rev. B **77**, 092409 (2008).
- ⁷Z. Q. Mao, T. He, M. M. Rosario, K. D. Nelson, D. Okuno, B. Ueland, I. G. Deac, P. Schiffer, Y. Liu, and R. J. Cava, Phys. Rev. Lett. **90**, 186601 (2003).
- ⁸S. Kimura, T. Takeuchi, K. Okunishi, M. Hagiwara, Z. He, K. Kindo, T. Taniyama, and M. Itoh, Phys. Rev. Lett. **100**, 057202 (2008).
- ⁹T. Yamauchi, Y. Ueda, and N. Mori, Phys. Rev. Lett. **89**, 057002 (2002).
- ¹⁰F. D. M. Haldane, Phys. Rev. B **25**, 4925 (1982).
- ¹¹K. Nomura and K. Okamoto, J. Phys. Soc. Jpn. **62**, 1123 (1993).
- ¹²T. Hikihara, M. Kaburagi, H. Kawamura, and T. Tonegawa, J. Phys. Soc. Jpn. **69**, 259 (2000).
- ¹³E. F. Bertaut, P. Blum, and G. Magnano, Bull. Soc. franç. Minér. Crist. **LXXIX**, 536 (1956).
- ¹⁴X. Zong, B. J. Suh, A. Niazi, J. Q. Yan, D. L. Schlagel, T. A. Lograsso, and D. C. Johnston, Phys. Rev. B **77**, 014412 (2008).
- ¹⁵J. M. Hastings, L. M. Corliss, W. Kunmann, and S. La Placa, J. Phys. Chem. Solids **28**, 1089 (1967).
- ¹⁶K. Yamaura, M. Arai, A. Sato, A. B. Karki, D. P. Young, R. Movshovich, S. Okamoto, D. Mandrus, and E. Takayama-Muromachi, Phys. Rev. Lett. **99**, 196601 (2007).
- ¹⁷S. Aasland, H. Fjellvåg, and B. Hauback, Solid State Commun. **101**, 187 (1997).
- ¹⁸H. Sakurai, Phys. Rev. B **78**, 094410 (2008).
- ¹⁹G. M. Kalvius, D. R. Noakes, and O. Hartmann, in *Handbook on the Physics and Chemistry of Rare Earths*, edited by K. A. Gschneidner, Jr., L. Eyring, and G. H. Lander (Elsevier Science, Amsterdam, 2001), Vol. 32, Chap. 206, and references cited therein.
- ²⁰If we fit the ZF spectrum of NaV_2O_4 using four independent initial phases (ϕ_i with $i=1-4$) in Eq. (2), we obtain $\phi_1 = -43(6)^\circ$, $\phi_2 = 20(6)^\circ$, $\phi_3 = -34(9)^\circ$, and $\phi_4 = 14(10)^\circ$ at 1.8 K. This would imply the possibility that the AF structure is not commensurate but incommensurate, although each ϕ_i is generally expected to be -45° for incommensurate magnetic order.
- ²¹O. Pieper, L. M. Corliss, W. Kunmann, and S. La Placa, Experimental Report of BENSFC, Report No. PHY-01-2088-EF, 2008 (unpublished).
- ²²J. Sugiyama, Y. Ikedo, P. L. Russo, H. Nozaki, K. Mukai, D. Andreica, A. Amato, M. Blangero, and C. Delmas, Phys. Rev. B **76**, 104412 (2007).